

## Supplementary Methods

### *Processing of OMVs preparations for transmission electron microscopy*

Purified OMV preparations were fixed using a solution of 2% paraformaldehyde and 2% glutaraldehyde for 30 minutes at 4°C. Samples were prepared by negative staining with 2.5% aqueous Uranyl Acetate stain (Agar Scientific, Stansted, UK), using the sequential drop method. Briefly, Carbon formvar TEM grids were pre-treated by glow discharging in air immediately prior to the adsorption of 5 µl of sample for 5 minutes. Grids were floated sample side down on two droplets of dH<sub>2</sub>O for 1 minute each followed by transfer to a droplet of stain for a further minute. Grids were retrieved and excess stain was wicked away with filter paper before being left to air dry.

Grids were imaged in a Zeiss Crossbeam 550 using the aSTEM1 detector and running SmartSEM software (Zeiss, Oberkochen, Germany) at 10.00kV accelerating voltage and images were collected at a nominal magnification of 60,000 X, to give pixel size of ~1 nm. Measurements were performed using the SmartSEM software.

## Supplementary Figure Legends

Supplementary Figure 1. Characterisation of generated OMVs for structural integrity and protein content

a) Analysis of structural integrity of OMVs using scanning electron microscopy. Images show structures of OMVs extracted from *A. baumannii* isolates BAL 084, BAL 191, BAL 215 and BAL 276, ranging in size from 20-100nm (Scale bar = 200nm). Micrographs were generated from a minimum of three individual OMV batches from an individual bacterial culture with a representative image shown. OMV size and structure is typical for previously published analyses of OMVs isolated from *A. baumannii* strains cultured from hospitalised patients<sup>1,2</sup>

b) OMV preparations were normalised to resolve 10µg of quantified protein content on SDS-PAGE gels visualised with Imperial protein stain. The typical resolved protein banding pattern from OMVs

isolated from BAL 276, BAL 191 and BAL 215. SDS-PAGE gels were generated from a minimum of three individual OMV batches from an individual bacterial culture with a representative image shown. Resolved proteins range in sizes indicated by protein standards.

Supplementary Figure 2. Sorting of OMV-specific B cells harvested from spleens of OMV-immunised Kymouse platform mice.

Panels show representative FACS plots rendered using FlowJo software (Becton Dickenson). Single splenocytes were gated using forward and side scatter channels and B cells were negatively selected using markers for CD8, CD4, Ly-6G, F4/80 and CD11c (all BV510). B cells negative for mouse lambda were gated on for B220 (BUV395), CD19 (BUV395) and for IgG (BV421). B cells expressing surface IgG were selected for binding of pooled OMVs generated from *A. baumannii* BAL 084, BAL 191, BAL 215 and BAL 276 stained with FM4-64 for sorting into single wells for paired IgH/L sequencing. FACS plot shown is representative of three individual experiments.

Supplementary Figure 3. Analysis of mAb binding to curated *A. baumannii* isolates clustered on human immunoglobulin heavy (H) and J chain (J) usage.

Curated collection encompasses CC2 typed isolates as well as other clonal complex typed isolates. IGHJ clustering shows convergence of IGHV2-5 IGHJ4 for CC2 cross-reactive mAbs (n=7) and the IGHV3-23 IGHJ2 (n=8) or the IGHV3-23 IGHJ4 germline genes (n=10) for mAbs specifically targeting KL49 producing CRAB isolates.

Supplementary Figure 4. Identification of Oxa-23 as the antigen targeted by mAbs 1348 and 1349.

a) Identification of antigen targets using serological expression cloning modified to screen for mAb reactivity. Upper panel shows reactive plaques generated by individual recombinant phage lambda containing random fragments of *A. baumannii* genomic DNA (Zap II) on nitrocellulose lifts from

plates of phage susceptible *E. coli* XL1B MRF'. Plaques 4, 5, 8 and 12 derive from recombinant phage lambda containing distinct sequences encoding expressible Oxa-23 reactive with mAbs 1348 and 1349. Lower panel shows nitrocellulose lifts incubated with unreactive mAbs.

b) Western blotting of whole bacterial cell lysates show mAb 1349 reacts with a single ~30 kDa protein band in bacterial lysates from BAL 084, BAL 191, BAL 215, and BAL 276, as well as from an additional Oxa-23 encoding *A. baumannii* (NCTC13424), but not an isolate lacking a class D  $\beta$ -lactamase (ATCC17978) or expressing class D  $\beta$ -lactamase Oxa-25 (NCTC13302). A similar binding pattern was observed with mAb 1348 by western blot. A representative blot is shown from a minimum of three individual experiments.

c) Western blotting of whole bacterial cell lysates show mAb 1042 reacts with a single ~10 kDa band in bacterial lysates from BAL 084, BAL 191, BAL 215, BAL 276, NCTC13424 and ATCC BAA-1710 but not ATCC17978. A similar binding pattern was observed with mAbs 1403, 1405, 1407, 1408 and 1413 by Western blot. A representative blot is shown from a minimum of three individual experiments.

Supplementary Figure 5. Identification of lipo-oligosaccharide (LOS) and capsule (K) as antigens targeted by selected mAbs

a) Carbohydrate extracts were generated from whole bacterial cell lysates. Left panel shows bacterial whole cell lysates resolved by SDS-PAGE and stained for protein. Right panel shows absence of resolved protein in the lysates after treatment with proteinase K representative of three individual experiments.

b) Western blotting of SDS-PAGE resolved carbohydrate extracts shows mAbs 1042 and 1407 bind a ~10-kDa band present in bacterial isolates producing LOS types as OCL1 but not OCL2 (ATCC17978). Similar binding patterns were observed with mAbs 1403, 1405, 1408 and 1413 by Western blotting of carbohydrate extracts. A representative blot is shown from a minimum of three individual experiments.

c) Western blotting of SDS-PAGE resolved carbohydrate extracts shows mAbs 1416 binds to a high molecular weight band present in carbohydrate extract generated from BAL 191 that produces capsule carbohydrate antigen typed as KL49, but not resolved carbohydrate extract generated from bacterial isolates producing distinctly typed capsule carbohydrate antigen. A representative blot is shown from a minimum of three individual experiments.

Supplementary Figure 6. Western blotting of whole bacterial lysates with selected mAbs reveals a high molecular weight band corresponding to capsule antigen in *A. baumannii* isolates that produce capsule carbohydrate antigen typed as KL49.

a) Western blotting of whole bacterial cell lysates from BAL 191 and additional *A. baumannii* isolates that produce capsule carbohydrate antigen typed as KL49, shows mAbs 1347 (RHS) and 1416 (LHS) bind to a high molecular weight band corresponding to resolved capsule antigen. A similar binding pattern was observed with mAbs 1345, 1350, 1351, 1363, 1364, 1397, 1398, 1400, 1401, 1402, 1404, 1409, 1410, 1412, 1414, and 1415 by Western blot. A representative blot is shown from a minimum of three individual experiments.

b) Western blotting of whole bacterial cell lysates from *A. baumannii* isolates that produce capsule carbohydrate antigen typed as KL49, shows no binding to a human IgG1 isotype control antibody suggested that binding to the high-molecular weight band was target specific. A representative blot is shown from a minimum of three individual experiments.

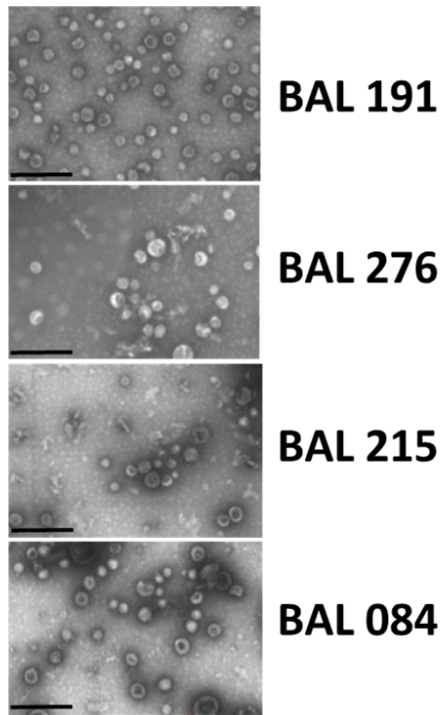
### Supplementary references

1. Mendez, J. A. *et al.* Extracellular Proteome of a Highly Invasive Multidrug-resistant Clinical Strain of *Acinetobacter baumannii*. *J. Proteome Res.* **11**, 5678–5694 (2012).
2. Kwon, S., Gho, Y. S., Lee, J. C. & Kim, S. I. Proteome analysis of outer membrane vesicles from a clinical *Acinetobacter baumannii* isolate. *FEMS Microbiol. Lett.* **297**, 150–156 (2009).

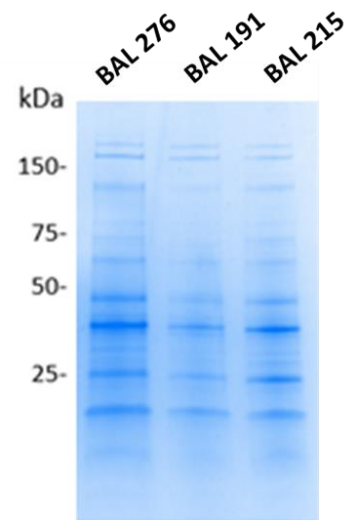


Supplementary Figure 1

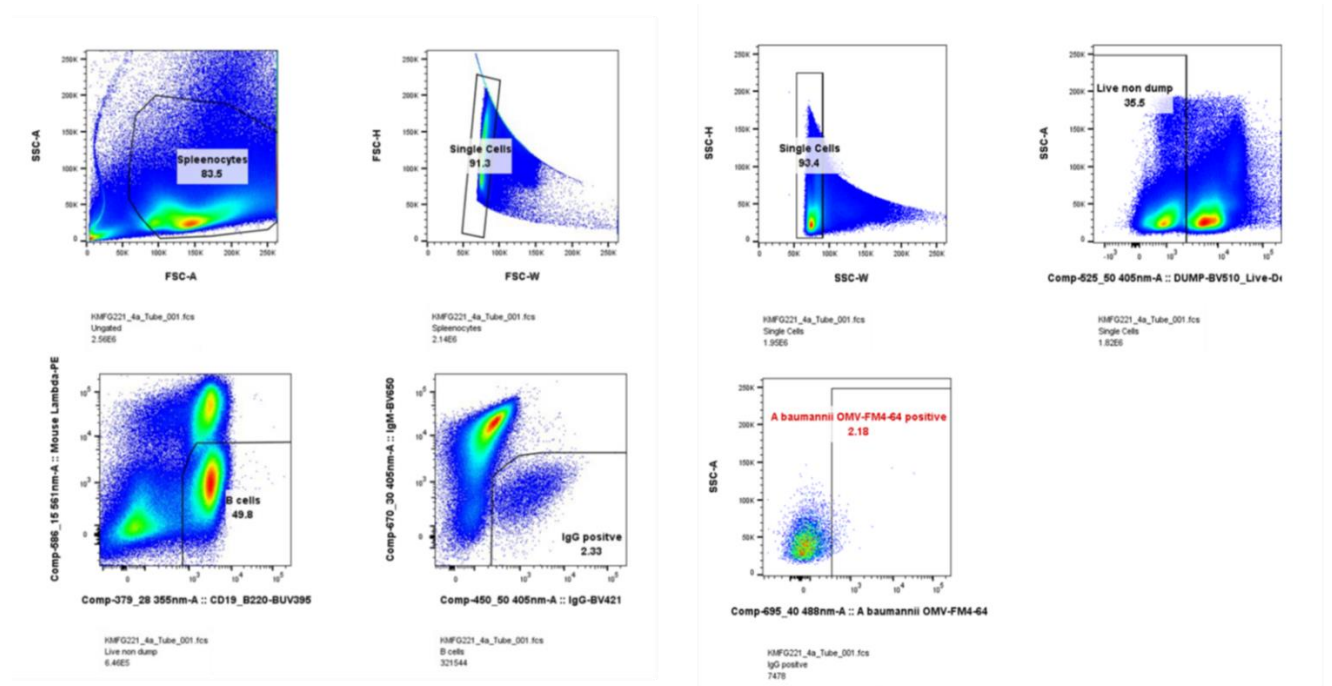
a)



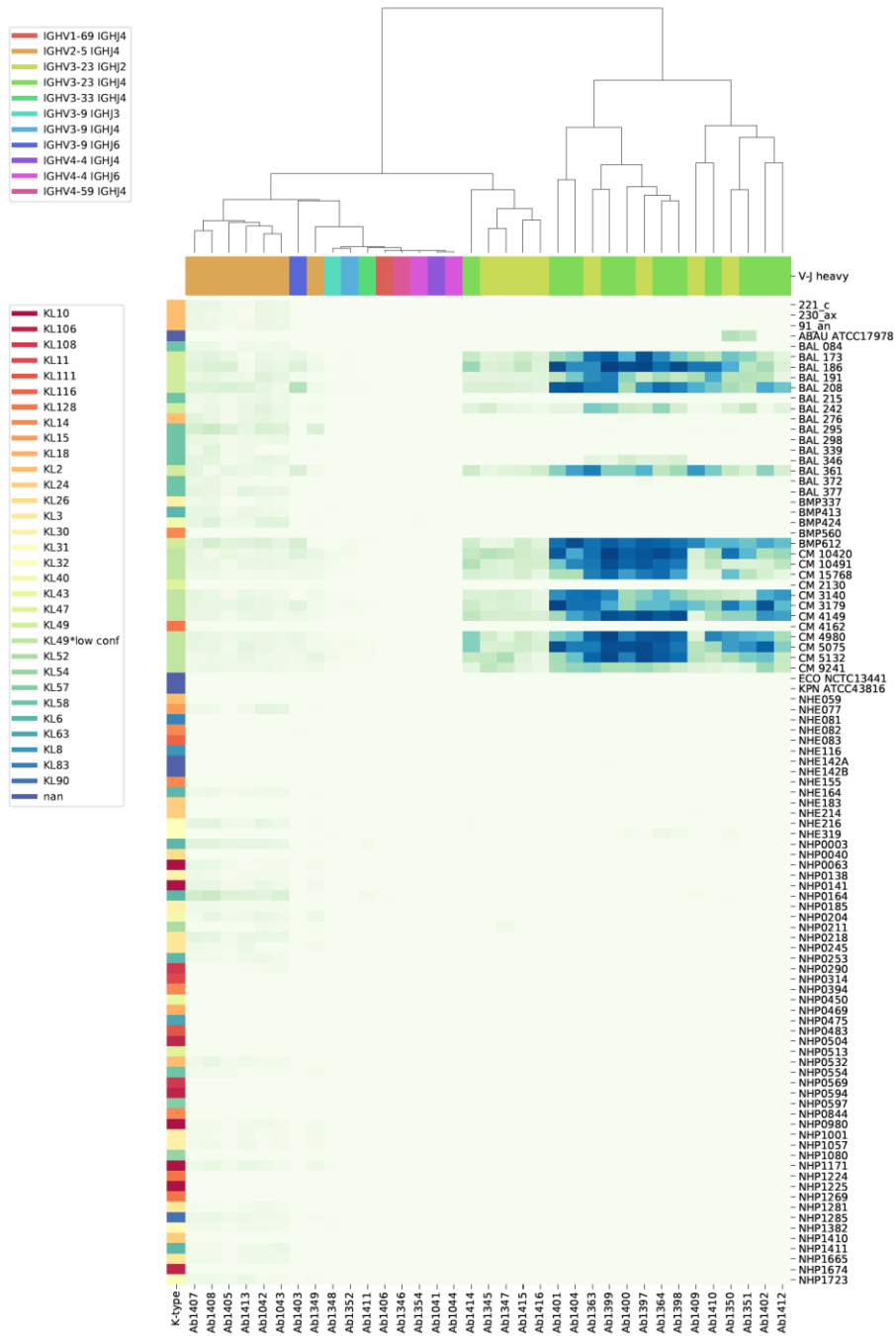
b)



## Supplementary Figure 2



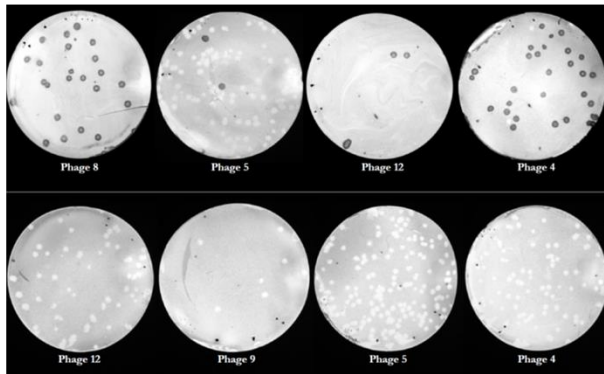
# Supplementary Figure 3



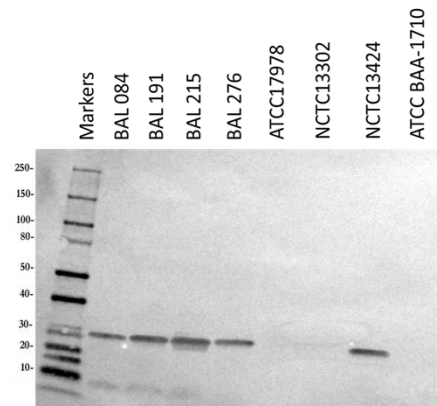


# Supplementary Figure 4

a)

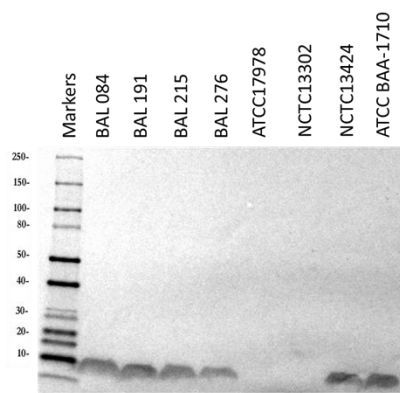


b)



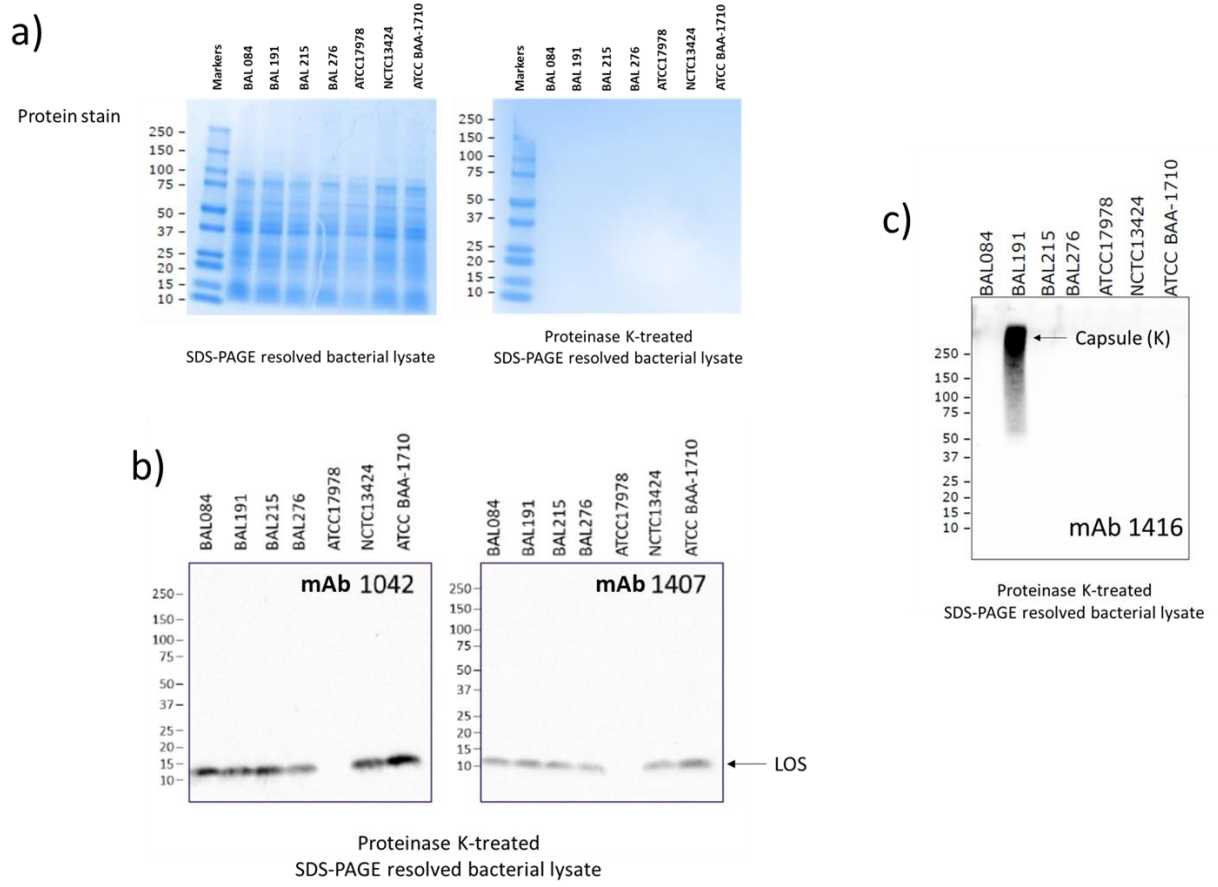
SDS-PAGE resolved Bacterial lysate

c)



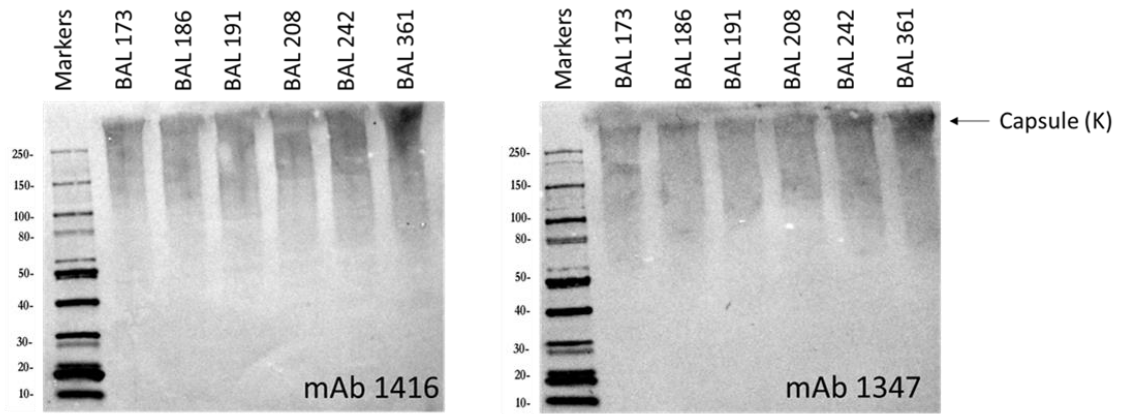
SDS-PAGE resolved Bacterial lysate

# Supplementary Figure 5



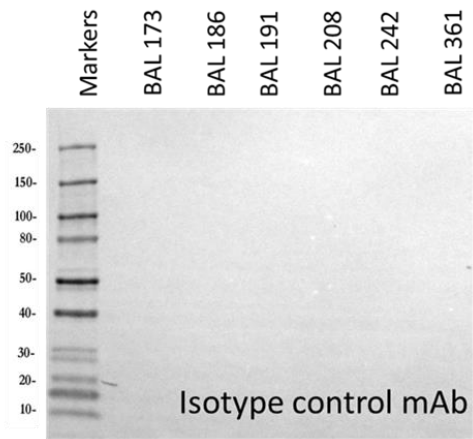
# Supplementary Figure 6

a)



SDS-PAGE resolved bacterial lysate

b)



SDS-PAGE resolved bacterial lysate

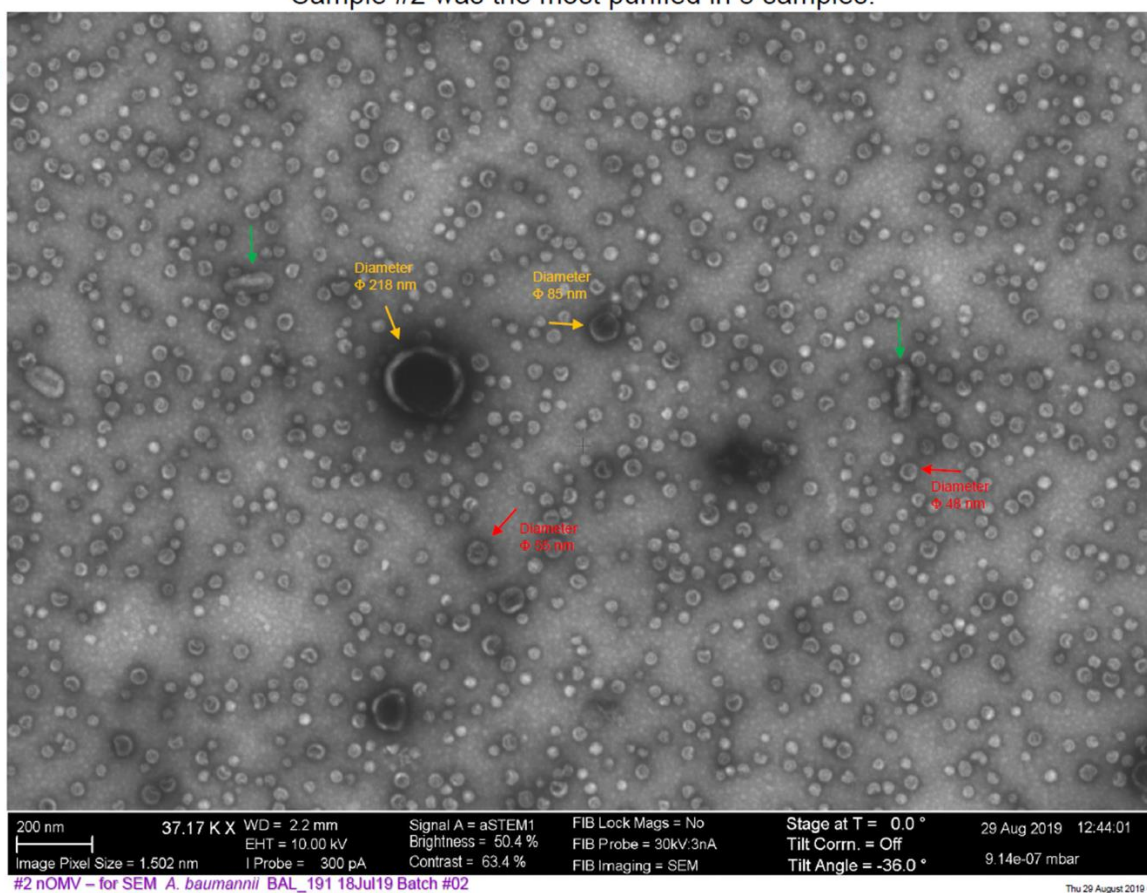
Uncropped image files

Supplementary Figure 1a

BAL 191

<Result> Sample NO.190828-#10 (STEM detector)  
Sample #2 was the most purified in 8 samples.

#10-1

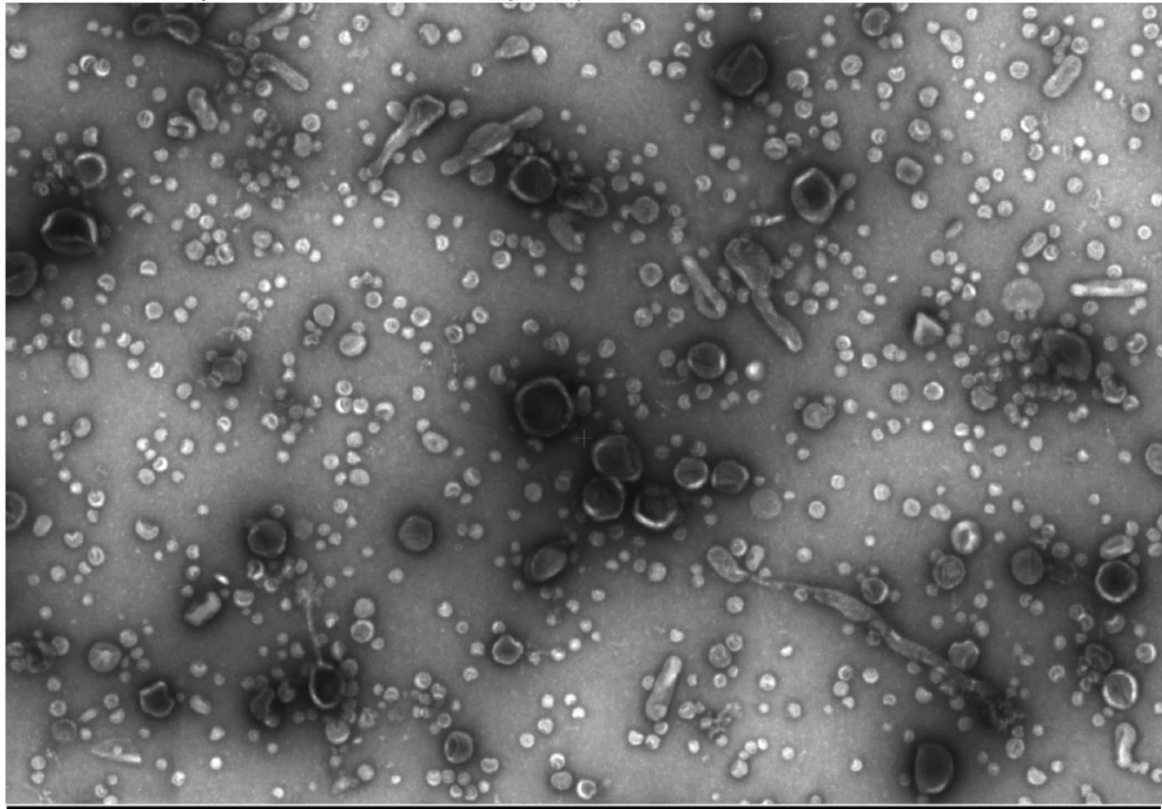


BAL 276

<Result> Sample NO.190828-#15 (STEM detector)

In Sample #7, there were Cherry-shape structures and some tail structures.

#15-2



200 nm	37.07 K X	WD = 2.3 mm	Signal A = aSTEM1	FIB Lock Mags = No	Stage at T = 0.0 °	29 Aug 2019 11:11:36
Image Pixel Size = 1.506 nm	EHT = 10.00 kV	Brightness = 50.0 %	FIB Probe = 30kV:3nA	Tilt Corr. = Off	Tilt Angle = -36.0 °	9.15e-07 mbar
I Probe = 300 pA	Contrast = 81.2 %	FIB Imaging = SEM				

#7 nOMV - for SEM *A. baumannii* BAL\_276 19Jul19 Batch #03

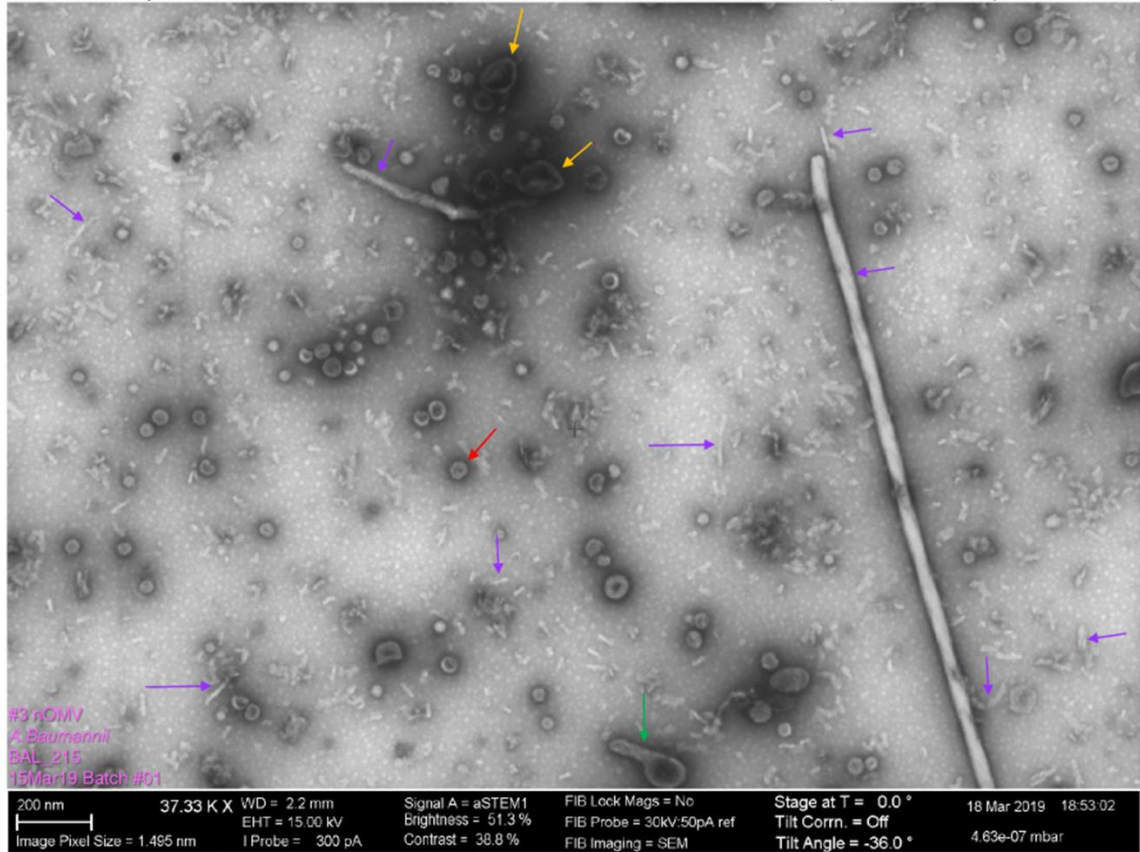
Thu 29 August 2019 Chieko Itakura

BAL 215

<Results-6> Sample NO.190318-#6 (STEM detector)

In Sample#3, there were also tuber structures or short sticks (50 – 100 nm)(Purple).

#6

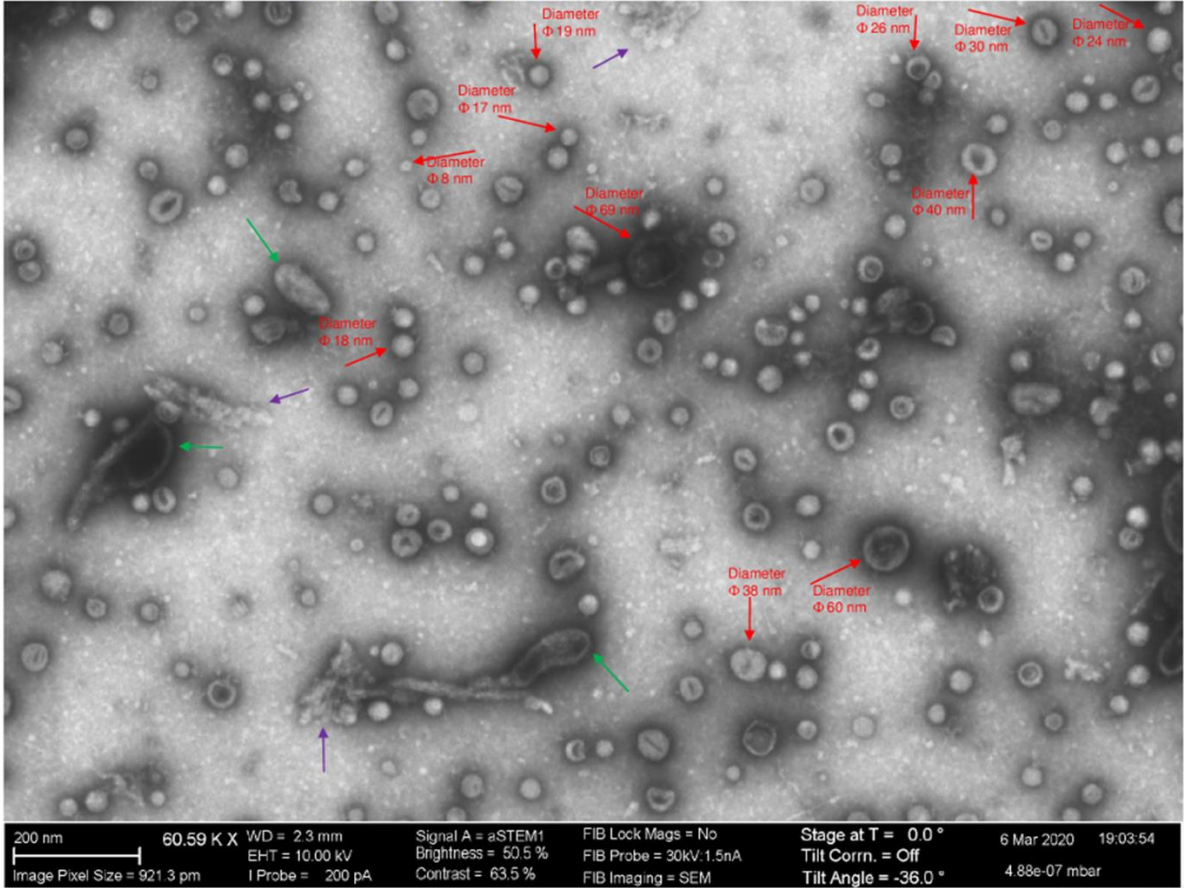


BAL 084

<Result> Sample NO.200305-#9 --- fixed with 2%GA+2%PFA #1

Sample #9 was not bad, but there were some aggregate marked purple arrows.

#9-7



Supplementary Figure 1b

